pH-Dependent Phase Behavior of Carbohydrate-Based Gemini Surfactants. Effect of the Length of the Hydrophobic Spacer

Jaap E. Klijn, Marc C. A. Stuart, Marco Scarzello, Anno Wagenaar, and Jan B. F. N. Engberts*

Physical Organic Chemistry Unit, Stratingh Institute, University of Groningen, 9747 AG Groningen, The Netherlands

Received: July 26, 2006; In Final Form: September 4, 2006

The phase behavior of a series of carbohydrate-based gemini surfactants with varying spacer lengths was studied using static and dynamic light scattering between pH 2 and 12. Cryo-electron microscopy pictures provide evidence for the different morphologies present in solution. The spacer length of the gemini surfactants was varied from two to 12 methylene units. At near neutral pH, spherical vesicles were obtained for gemini surfactants with a spacer shorter than 10 methylene units, whereas nonspherical vesicles were obtained for spacer lengths of 10 and 12. Upon decreasing the pH, the vesicles underwent transitions toward worm-like micelles and spherical micelles for a spacer length of six and larger, whereas for shorter spacers, these transitions are not observed. For the shortest spacer at low pH, perforated vesicles are observed, and vesicles built from the gemini surfactant with a spacer of four methylene units only underwent a transition toward worm-like micelles. Upon increasing the pH to slightly basic values, flocculation followed by redispersion upon charge reversal was observed up to a spacer length of eight methylene units. The redispersal is explained by hydroxide-ion binding to the uncharged vesicular surface. By contrast, vesicles formed from the gemini surfactants with 10 and 12 methylene units only undergo a transition toward inverted phases. The observations can be understood in terms of the packing parameter.

Introduction

When two classical surfactants are covalently linked through a spacer, gemini surfactants are obtained.[1] Recently, gemini surfactants with two tertiary amine functionalities and carrying (reduced) carbohydrate units bound to the headgroups (Scheme 1A) have been synthesized as nonviral gene-delivering vehicles.[2,3] In the absence of DNA, they display an amazingly rich phase behavior, not only upon variation of the headgroup and spacer[4,5] but also in mixtures with other vesicle- and micelle-forming amphiphiles.[6] Depending on the pH, both, one, or neither of the two nitrogen atoms is protonated. At a high degree of protonation, aggregates with high curvatures are formed, whereas at low degrees of protonation, aggregates with lower curvatures such as vesicles and oil droplets are observed.[4−6] Interestingly, upon charge neutralization of the cationic vesicles and of oil droplets, hydroxide ions are specifically adsorbed at the aggregate/water interface at slightly basic pH.

For a typical carbohydrate-based gemini surfactant, unilamellar vesicles can be formed at near neutral pH.[7] Morphological transitions are observed by static and dynamic light scattering and confirmed by cryo-electron microscopy. Decreasing the pH leads to the gradual formation of worm-like micelles, initially coexisting with the remaining vesicles. The transition is accompanied by a strong decrease in the intensity of scattered light and a decrease of the maximum in the observed size distribution. At a specific pH (typically around pH 6), the conversion is completed as evidenced by a low but constant intensity of scattered light. Further lowering the pH by one unit results in the transformation of worm-like micelles into spherical micelles, and the intensity of scattered light finally drops to a value close to the background signal.

SCHEME 1: General Structure of Previously Studied Gemini Surfactants (n = 0, 1)[a]

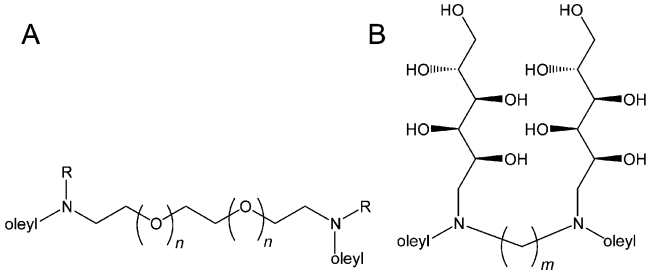

[a] (A) R can be a methyl, a reduced monosaccharide, or a methyl-terminated oligo(ethylene oxide). In panel B, the gemini surfactants presented here are shown. The value of m can be 2 (**1**), 4 (**2**), 6 (**3**), 8 (**4**), 10 (**5**), or 12 (**6**).

Upon going in the opposite direction (i.e., from neutral pH going up), the electrostatic repulsion between vesicles is gradually lowered, ultimately leading to flocculation of the vesicles. However, at an even more basic pH, they redisperse with the same vesicular size distribution as before flocculation due to specific adsorption of hydroxide ions. These effects have been discussed in detail in previous papers.[4,5]

Here, we present the results for a series of gemini surfactants of which the size of the hydrophobic spacer is varied between two and 12 carbon atoms (Scheme 1B; $m = 2-12$). It is known that for gemini surfactants with bisquaternary ammonium headgroups, the cmc increases with increasing spacer length but decreases again above a spacer length of about six carbon atoms.[8,9] However, when the surface area of the surfactant at

* Corresponding author. E-mail: J.B.F.N.Engberts@rug.nl.

10.1021/jp064774z CCC: $33.50
Published on Web 10/11/2006

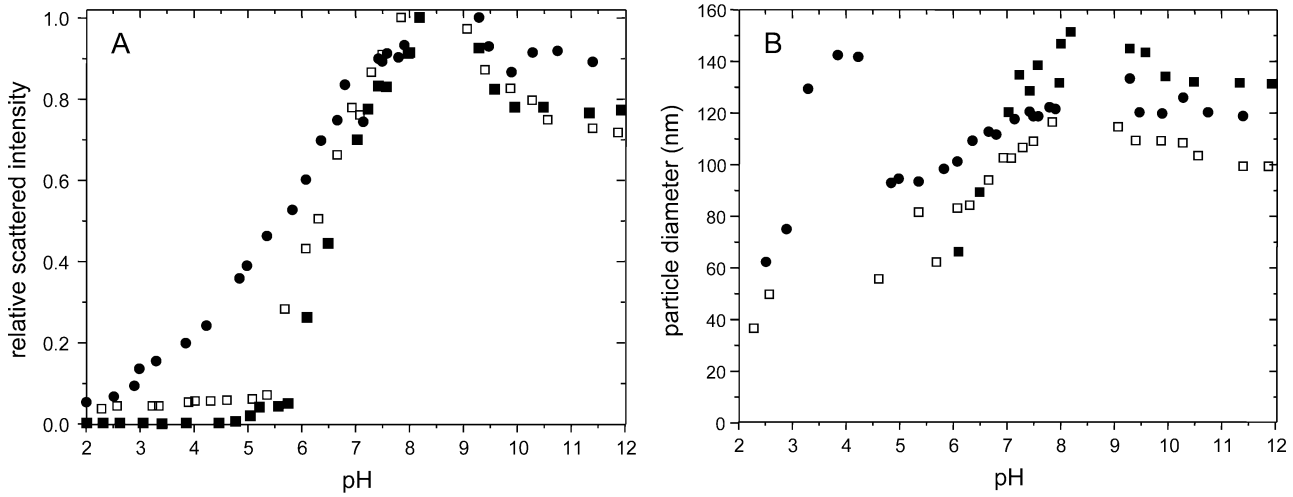

Figure 1. Relative scattered intensity (A) and size distributions (B) of solutions containing gemini amphiphile **1** (●), **2** (□), and **3** (■) as a function of pH. For clarity, in panel B only the maximum in the size distribution is given. Between approximately pH 8 and 9, data could not be obtained due to phase separation.

the air−water interface is considered, the decrease starts at about 10 carbon atoms in the spacer. This suggests that the spacer begins to contribute to the hydrophobic volume only at more than six carbon atoms but that back-folding of the spacer into the hydrophobic interior of the aggregate does not occur until the spacer contains 10 carbon atoms. For the systems under study here, these observations are important since the length of the spacer will affect both the pK_a values of the nitrogen atoms as well as the average packing parameter.

The packing parameter *P*, developed by Israelachvili and Ninham,[10] is helpful in explaining the observed phase behavior. This parameter provides a prediction of the morphology of the aggregate by approximating its surface curvature.

$$P = \frac{V}{a_0 l_c} \tag{1}$$

In this equation, V is the volume of the hydrophobic part of the molecule, a_0 is the mean cross-sectional headgroup surface area, and l_c is the length of the extended all-trans alkyl tail. For a small packing parameter (<1/3), the shape of the surfactant favors a large positive curvature, leading to small aggregates (spherical micelles). Between a value of one-third and one-half, worm-like micelles are usually formed, and vesicles are observed when the packing parameter is between one-half and 1. In the case of a large packing parameter (>1), there is a negative curvature leading to inverted structures (e.g., hexagonal, cubic, etc.).

Experimental Procedures

Materials. Gemini surfactants were synthesized as described previously.[7] Detailed synthetic procedures will be reported in a forthcoming paper.[11] Hepes, Mes (4-morpholinoethanesulfonic acid), APS (3-amino-1-propanesulfonic acid), and taurine (2-aminoethanesulfonic acid) were purchased from Sigma and used as received.

Sample Preparation. Solutions of gemini surfactant in chloroform were dried under a stream of nitrogen. Traces of residual solvent were removed under vacuum. To obtain small unilamellar vesicles (SUVs) with a narrow and reproducible size distribution, the lipid films were hydrated at room temperature in bidistilled water containing 5 mM each of the buffer substances Hepes, Mes, and taurine and 10 mM of APS at a pH close to the pH of flocculation of the gemini surfactant being studied (unless stated otherwise), vortexed for several minutes, briefly tip-sonicated (<30 s), freeze−thawed [N_2(l) ↔ water bath (40 °C)] 5 times, and extruded 11 times through a 200 nm pore-size polycarbonate filter. Typically, this procedure leads to vesicles with a maximum in the size distribution of about 150 nm.

The samples for light scattering measurements were prepared by diluting the 5 mM (total lipid concentration) vesicular stock solutions to a final concentration of 0.25 mM and adding a few microliters of HCl (aq) (ca. 4 M) or NaOH (aq) (ca. 2 M) to obtain the desired pH. The dispersions were allowed to equilibrate overnight before measuring.

Static and Dynamic Light Scattering. Static and dynamic light scattering measurements were performed at 25 °C on a Zetasizer 5000 instrument (Malvern Instruments) at $\lambda = 633$ nm. To obtain the hydrodynamic radii, the intensity autocorrelation functions were analyzed using CONTIN. The obtained intensities from static light scattering experiments were normalized against the maximum scattered intensity for that particular gemini surfactant. The experimental data of experiments was normalized such that the curves overlap and the pH values of the transitions are most clearly displayed. Note that trends in scattered intensities are meaningful but that absolute values of scattered intensities obtained solely from larger structures (vesicles, inverted phases) are relatively meaningless.

Cryo-Transmission Electron Microscopy. A drop of the lipid suspension was deposited on a glow discharged holey carbon-coated grid. After blotting away the excess of lipid, the grids were rapidly plunged into liquid ethane. The frozen specimen were mounted in a Gatan (model 626) cryo-stage and examined in a Philips CM 120 cryo-electron microscope operating at 120 kV. Micrographs were recorded under low dose conditions.

Results and Discussion

Six Carbon Spacer (3, $m = 6$). The phase behavior of **3** ($m = 6$) closely resembles that of previously described gemini surfactants, and therefore, its behavior will not be described extensively.[4,6] The only difference is that the pH of the transitions occurs at slightly different pH values (Figure 1). For these reasons, we take **3** as a starting point since the aggregation behavior of **3** is well-defined and observed effects upon varying the spacer length are easiest explained and understood starting from **3**.

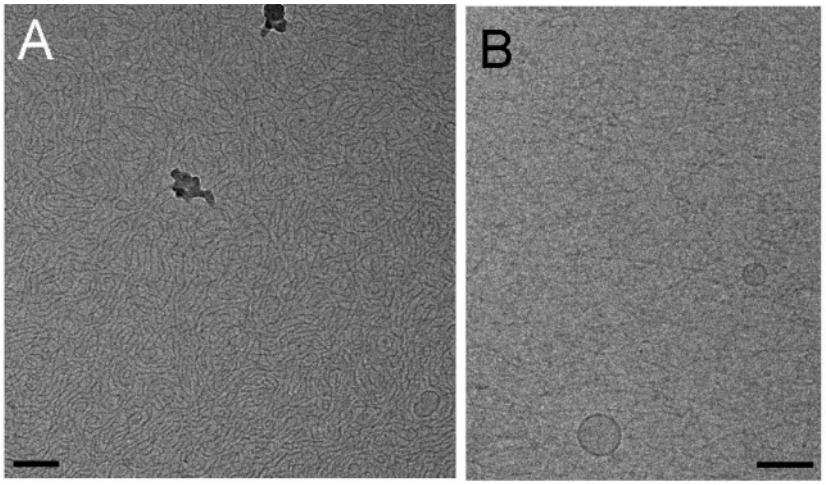

Figure 2. Cryo-electron microscopy pictures of **2** at pH 4.9 (panel A: after equilibration overnight) and pH 2.1 (panel B: 1 h equilibration). See text for explanation. The bar represents 100 nm.

Four Carbon Spacer (2, $m = 4$). Amphiphile **3** has an *n*-hexyl spacer, and decreasing the size of the spacer to four methylene units ($m = 4$) does not lead to a change in the pH at which the vesicles flocculate upon increasing the pH of a vesicular dispersion prepared at pH 7.5. This is expected since under these circumstances, the few remaining charges are too far separated to influence each other, and hence, removal of the last protons is not affected by a decrease in spacer length.

On the contrary, decreasing the pH starting from a low positive surface charge, the pH values of structural transitions are significantly affected by a decrease in the size of the alkyl spacer. Whereas **3** forms spherical micelles at pH 4.9, this is not the case for **2**. At pH 5.5, the scattered intensity of **2** levels off to a plateau value, which, in the case of gemini surfactants with an *n*-hexyl or oligo(ethylene oxide) spacer, corresponds to the presence of worm-like micelles.[4,6] Below pH 3.7, this low intensity of scattered light decreases further as a function of time, suggesting the onset of slow morphological transitions. This behavior is in contrast to observations made for other gemini surfactants, but clearly, further work is necessary to clarify the origin of the phenomenon (Supporting Information).

To obtain more information on the pH-induced morphological changes of the aggregates formed from **2**, cryo-electron microscopy pictures were taken. At pH 7.7 and 6.4, only vesicles are observed, although the vesicles are largely nonspherical (elongated) at pH 6.4 (Supporting Information). Similar morphologies have been observed for vesicles in transition toward worm-like micelles.[12,13] Indeed, at pH 4.9, worm-like micelles are observed. This is also true at pH 2.1. However, also a few small vesicles are still visible.

The observations that the transitions toward structures with higher curvatures than those of vesicles occur for **2** at lower pH values can be rationalized considering two things. First, the packing parameter of the gemini surfactants at the same protonation state increases going from **3** to **2** due to a decrease in surface area. This means that to obtain the same packing parameter for both surfactants, amphiphile **2** needs to be protonated to a higher extent since protonation leads to an increase in surface area because of stronger intraheadgroup electrostatic repulsion and more extensive headgroup hydration. Second, double protonation of **2** will occur at a lower pH due to an increase in intramolecular electrostatic repulsion as a result of the first protonation step.

Two Carbon Spacer (1, $m = 2$). Similar as for the change from six to four methylene units in the spacer, a further decrease in spacer length to two methylene units (**1**; $m = 2$) does not affect the pH of flocculation and redispersion. Furthermore, double protonation is further hampered as can be seen from the relatively high scattered intensities and particle diameters at low pH (Figure 1). In contrast to **2**, no time dependence of the scattered intensity and particle diameter was observed (data not shown).

Upon lowering the pH, the behavior of **1** is similar to that of **2** and **3**, except that the decrease in scattered intensity and particle diameter occurs over a broader pH range. For **3** below pH 4.9, only spherical micelles are present, whereas for **1**, this is the pH at which the average size increases again, until a maximum is reached between pH 4.2 and 2.8. When this maximum is reached, the linear decrease in count rate shows a break. This clearly demonstrates the occurrence of rather complex morphological changes.

Again, cryo-electron microscopic pictures were taken to further clarify these pH-induced effects. At pH 10.2 and 6.7, only (spherical) vesicles are observed (Supporting Information). However, at pH 4.9, the vesicle surface becomes less smooth, and also bilayer fragments are observed (Supporting Information). A further decrease in pH to 3.4 leads to even less smooth vesicular surfaces (Figure 3A). In addition, the top side of the vesicles shows darker and brighter areas, indicating the presence of small holes in the membrane (<10 nm). This effect is even more pronounced at pH 2.1 and 1.1 (Figure 3B,C). Vesicles containing large numbers of small holes (perforated vesicles) have been observed previously as intermediate structures in the transition of vesicles into mixed globular micelles induced by the addition of charged detergents.[14−17]

It is likely that perforated vesicles are close in morphology to branched and multi-connected worm-like micelles. At pH 1.1, perforated vesicles are observed again but now in coexistence with worm-like micelles (Figure 3C). However, these worm-like micelles are much longer than the ones typically observed (e.g., **2**; Figure 2).

Eight and 10 Carbon Spacer (4, $m = 8$ and 5, $m = 10$). We now turn our attention to spacer lengths larger than that of **3**. Increasing the size of the spacer from six to eight methylene units (**4**; $m = 8$), the pH at which vesicles flocculate and redisperse, increases to 8.6 and 9.9, respectively (Supporting Information), whereas the other transitions are only slightly affected. Increasing the length of the spacer to 10 methylene units (**5**; $m = 10$) leads to a situation that the absolute scattered intensity increased to higher values than that observed for the

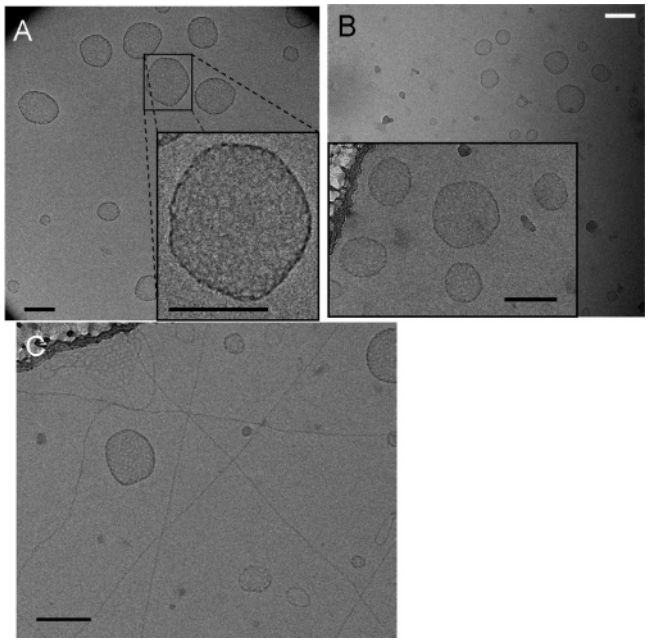

Figure 3. Cryo-electron microscopy pictures of **1** equilibrated overnight at pH 3.4 (A), pH 2.1 (B), and pH 1.1 (C). See text for explanation. Bar represents 100 nm.

gemini surfactants with a shorter spacer (Figure 4). Furthermore, attempts to prepare the solutions above pH 8.0 failed due to phase separation.

Cryo-TEM pictures of **5** at pH 7.4 do not only show spherical vesicles (Figure 5B) but also show elongated vesicles and vesicles just touching each other in a very small area, apparently in the process of fusion. Also, large elongated vesicles are found (Supporting Information). Considering that dynamic light scattering experiments indicate particles with diameters around 150 nm at this pH, it seems unlikely that these assemblies exist in large amounts in bulk solution. Therefore, it appears more likely that vesicles formed from **5** are only sensitive toward fusion and that the observed morphologies are formed due to the enforced accumulation of aggregates, typical for the conditions of cryo-electron microscopy experiments.[13]

The process of spontaneous fusion requires areas in the membrane with negative curvature (Figure 5B) (i.e., surfactants with a packing parameter larger than 1). Since **5** has a tendency towards vesicular fusion, it seems likely that the packing parameter at about pH 7.5 is close to 1. As noted previously for gemini surfactants with bisquaternary ammonium headgroups, the spacer begins to contribute to the hydrophobic volume for a length greater than six, but it does not fold back until it reaches a length of 10 carbon atoms.[8,9] Of course, these observations may not necessarily hold for the present gemini surfactant, but considering the phase behavior of **5**, it looks likely that the anticipated increase in surface area relative to that of **4** is well-compensated by an increase in the hydrophobic volume.

Indeed, when the pH is increased from 7.4 to 8.3, thus further increasing the packing parameter of **5**, inverted phases, presumably cubic, are formed (Figure 5C). In addition, some vesicles in the process of forming inverted phases can be seen (L_3 phase).[19,20] Decreasing the pH from 7.4 to 6.8 leads to the formation of ellipsoidal vesicles as expected for a lowering of the packing parameter (Figure 5A).

Twelve Carbon Spacer (6, $m = 12$). Finally, the length of the alkyl spacer was increased to 12 methylene units (**6**, $m = 12$). It is expected that this compound behaves similarly to **5**, except that the hydrophobic spacer contributes to a larger extent to the hydrophobic volume (i.e., leading to a still larger packing parameter). Hence, both the formation of inverted phases and the presence of spherical vesicles are expected to occur at lower pH values than for **5**.

Unfortunately, the experimental data for **6** are somewhat less reproducible than those for the other gemini surfactants. Nevertheless, the transitions could be identified (Figure 6). Considering the average particle size, the behavior at acidic pH is similar for independent experiments performed with **6**. Some experiments were performed starting from low pH (<4.5) and then going up in pH without the external input of significant amounts of mechanical energy. This also led to the formation of large aggregates. Similar experiments have been performed previously[5] with gemini surfactants that are liquid at room temperature, and in those cases large, homogeneous aggregates (oil droplets) have been observed.

To address the structural transitions, cryo-electron microscopy pictures of solutions at various pH values were taken (Figure 7). At pH 6.3, vesicles are observed that have an irregular surface, similar to those observed for **5** at pH 6.8 (Figure 5A). At pH 7.1, elongated vesicles can be seen together with vesicles with large holes (20−50 nm). Pictures taken at pH 8.5 (Figure 7C) reveal the presence of almost spherical particles that are close to being homogeneous in nature but less homogeneous than what has been observed previously for oil droplets (i.e., no bilayers are observed, and the interior of the particle has a darker color than the surrounding water).[5] Since **6** is not a liquid at room temperature and since the phase behavior of **6** is similar to that of **5**, we suspect that the aggregates reside in an inverted phase. However, this inverted phase is probably different from the one observed for **5** as indicated by the cryo-electron microscopy pictures.

Effects of Spacer Length Variation. Figure 8 summarizes the pH of the transitions for the gemini surfactants with spacer lengths varying from 2 to 12. For spacers of $m = 10$ and 12, the symbol × denotes, going up in pH, a transition from lamellar to inverted structures, and for $m = 2$ going down in pH a transition from vesicles to perforated vesicles. The large error for this transition is based on the pH values at which cryo-electron microscopy pictures were taken since the intensity of scattered light and the size distributions did not clearly reveal where this transition occurs. Despite the fact that aggregates of the same phase, but of different morphology, such as spherical vesicles (**1**; pH 6.7) and irregularly shaped vesicles with 30 nm holes (**6**; pH 7.1), are observed, the pH of the same phase transitions could be determined as described previously.[4,6]

The effects of a varying spacer length on the transition are rather complex as both the surface area and the hydrophobic volume are affected. From eq 1, it can be seen that changes in these parameters can both enhance and compensate each other. In addition, the degree of protonation of the amine functionalities depends on the spacer length as well.

From the literature,[8,9] it is known that an increase in the length of the spacer of gemini surfactants leads to an increase in the surface area. Hence, the packing parameter at the same degree of protonation decreases (eq 1; Figure 9). However, at a certain length, the spacer will contribute to the hydrophobic volume compensating for the increase in surface area. This leads to a smaller decrease or even an increase in the packing parameter. Upon further increasing the length of the spacer, the spacer will fold back into the hydrophobic domain leading to a decrease in the surface area. Then, there are a number of possibilities, but most likely, from the results obtained (vide infra), the packing

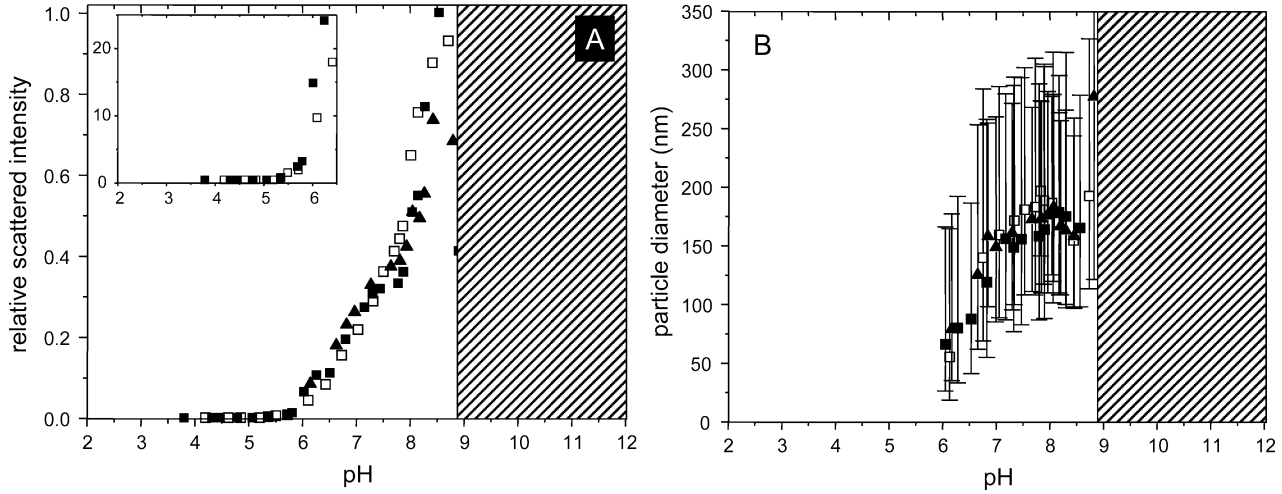

Figure 4. Experimental data for solutions containing **5**. Error bars denote the width of the size distribution.[18] Solid and open symbols represent independent experiments starting from stock solutions prepared near neutral pH. Lined bar denotes the pH region where data could not be obtained due to phase separation. The insert in panel A displays the absolute scattered intensity.

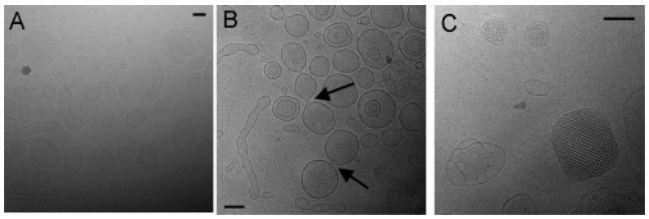

Figure 5. Cryo-electron microscopy pictures of **5** equilibrated overnight at pH 6.8 (A), pH 7.4 (B), and pH 8.3 (C). See text for explanation. Arrow indicates some areas with negative curvature. Bar represents 100 nm.

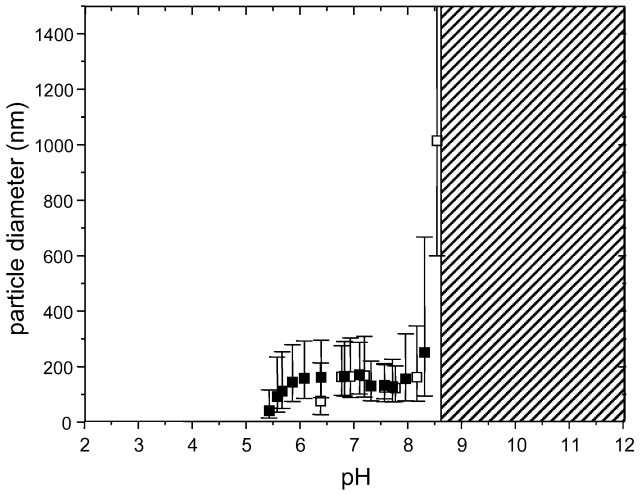

Figure 6. Size distributions of solutions containing gemini amphiphile **6** as a function of pH. For legend details, see Figure 4.

parameter at the same protonation state will increase or increase more strongly upon elongation of the spacer than before.

In the system under study, it is difficult to determine exactly at which spacer length back-folding starts. Spacers with $m < 6$ cannot fold back into the hydrophobic volume. Considering that the formation of inverted phases ($P > 1$) can only result from an increase in the hydrophobic volume and/or a decrease in the average cross-sectional headgroup area, it seems reasonable that at low degrees of protonation, back-folding occurs for $m > 8$. However, this observation does not exclude back-folding for $m = 6$ and 8. If at higher degrees of protonation back-folding can be related to maxima in the pH of the phase transitions, then back-folding begins at $m > 8$.

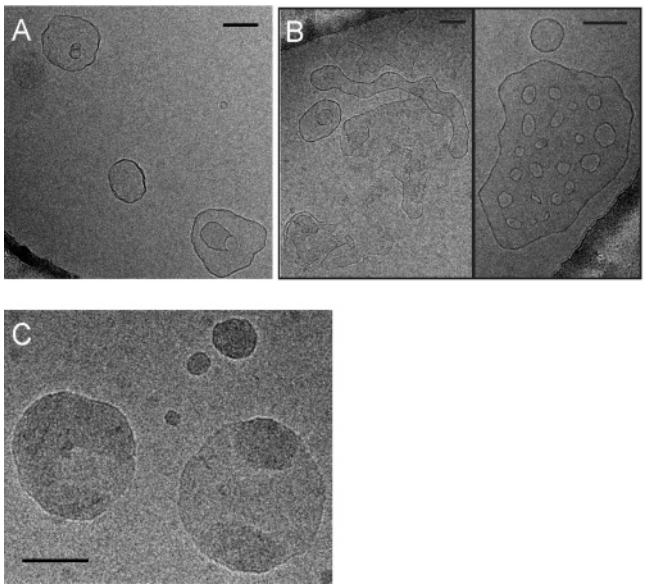

Figure 7. Cryo-electron microscopy pictures of **6** equilibrated overnight at pH 6.3 (A), pH 7.1 (B), and pH 8.5 (C). See text for explanation. Bar represents 100 nm.

Starting from $m = 6$, decreasing the length of the spacer results in a strong decrease of the pH at which spherical micelles transform into worm-like micelles to values below 2. If it is assumed that the transition from spherical to worm-like micelles requires the same value of the packing parameter for all gemini surfactants, the decrease in spacer length, leading to an increase in the packing parameter at the same protonation state, alone cannot explain this large effect. Considering that this transition is associated with a high degree of protonation of the gemini surfactants suggests that the pK_a values of at least one of the nitrogen atoms is significantly decreased.

Upon increasing the spacer length from $m = 6$ to $m = 12$, the pH of the transition from spherical micelles to worm-like micelles is only weakly affected.

The intermolecular N−N distance of the gemini surfactants at the aggregate surface (Scheme 2) is determined by a balance of repulsive forces between headgroups of neighboring gemini surfactants in the aggregate and attractive van der Waals forces. This distance adapts itself as a response to external stimuli (e.g., changes in the degree of protonation). For spacers longer than the intermolecular N−N distance, the intramolecular N−N

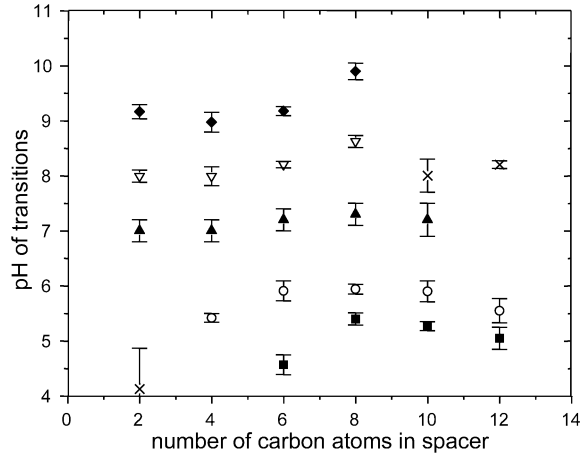

Figure 8. Plot of the pH of the transitions as a function of the length of the spacer. The ▲ indicates the pH at which worm-like micelle formation from vesicles starts, ○ indicates the pH at which the formation of spherical micelles from worm-like micelles starts, ■ indicates the highest pH at which only spherical micelles are observed, ▽ indicates the pH of flocculation, ◆ indicates the pH of redispersion, and × indicates a transition specified in the text.

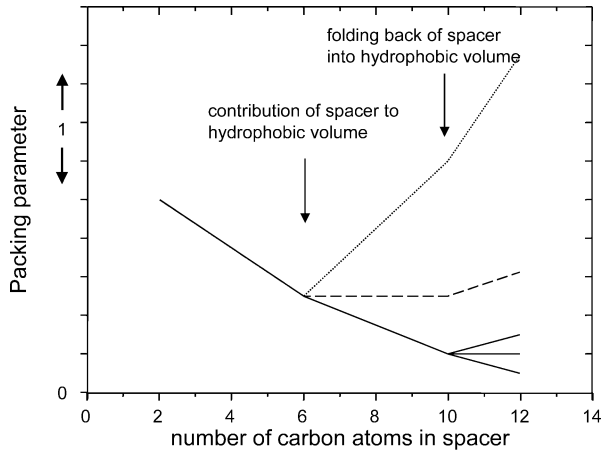

Figure 9. Trends in the packing parameter at the same protonation state as a function of the spacer length for changes in hydrophobic volume and surface area. The values on the *y*-axis depend on the protonation state but range from 0 to values close to 1.[21] The magnitude of the slopes of the lines is arbitrarily chosen. The location of the breaks in the plot are based on literature observations (see text).[8,9]

SCHEME 2: Schematic Presentation of the Dependence of the pK_a Values on the Length of the Spacer for a Long (Left) and a Short (Right) Spacer[a]

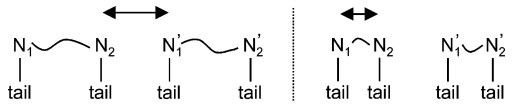

[a] The arrows denote the shortest N−N distance.

distance is determined in a similar way, and therefore, it will be at least as long as the intermolecular N−N distance. At high degrees of protonation, neighboring surfactant molecules then largely determine the pK_a value of the second nitrogen atom. Hence, this largely explains the constant pH for the transition from spherical micelles to worm-like micelles for gemini surfactants with $m \geq 6$. On the contrary, when the spacer is shorter than the intermolecular N−N distance, the intramolecular distance will then mainly determine the pK_a value of the second nitrogen atom. Consequently, the pK_a value of the second nitrogen atom will decrease. This leads to the conclusion that at the surface of spherical micelles,[22] the intermolecular N−N distance is about equal to the intramolecular N−N distance in **2** and **3** since the pH of the transition drops strongly going from $m = 6$ to $m = 4$.

Similarly, the pH of the transition from worm-like micelles to vesicles strongly drops below a spacer length of $m = 4$. One could argue that the packing parameter of the gemini surfactants forming perforated vesicles is close to the packing parameter in worm-like micelles,[14−17] but nevertheless, it is justified to conclude that in worm-like micelles, the intermolecular nitrogen distance is about the same as the intramolecular nitrogen atom distance in **2**. This is in agreement with the lower degree of protonation in worm-like micelles and hence weaker electrostatic repulsion between the nitrogen atoms of neighboring gemini surfactants.

Upon going from $m = 2$ to $m = 8$, the pH of flocculation increases only by about 1 pH unit. Flocculation is related to removal of the last protons from the surface leading to a low positive zeta potential.[7,23] Hence, neighboring charges are too far apart to be affected by one another. As a consequence, changes in the pH of flocculation are more likely due to (small) changes in the hydration of the interface. The pH of redispersion, coming from adsorption of hydroxide ions to the interface,[7,23] is affected in a similar way as the pH of flocculation. However, for spacers with $m > 8$, no redispersion is observed due to the formation of inverted phases.

Conclusion

A detailed study of the pH-dependent phase behavior of a series of carbohydrate-based gemini surfactants with varying lengths of the hydrophobic spacers (*m*) has been performed. The pH has been varied between pH 2 and 12, leading to different degrees of protonation of the amine functionalities in the surfactant headgroup. The series contains gemini surfactants with a hydrophobic spacer varying in length between two and 12 methylene units.

The transitions from vesicles toward aggregates of higher curvatures, such as the transitions from vesicles to worm-like micelles and from worm-like to spherical micelles, are strongly affected for spacers of $m < 6$. If *m* is 2 and 4, no spherical micelles are observed in the pH range studied, and the same holds for worm-like micelles for a spacer of $m = 2$. Instead, for $m = 2$, perforated vesicles are observed, which can be seen as branched and multi-connected worm-like micelles. The decrease in the pH of these transitions is the result of an increase of the packing parameter at the same protonation state upon decreasing values of *m*. As a consequence, a higher degree of protonation is required to observe the structural transitions. However, for $m = 2$ and 4, the intramolecular N−N distance becomes smaller than the intermolecular N−N distance leading to hampering of double protonation. Therefore, it can be concluded that the intermolecular N−N distance in spherical and worm-like micelles is comparable to the intramolecular N−N distance of gemini surfactants with $m = 6$ and 4, respectively.

Almost complete deprotonation of the amine groups at the vesicular surface occurs at pH 8 and is rather independent of the length of the spacer (only 1 pH unit increase going from $m = 2$ to 8). Adsorption of hydroxide ions to the vesicular surface starting at pH 9 follows the same trend. Interestingly, for spacers with $m = 10$ and 12, inverted phases are formed, consistent with back-folding of the spacer.

Acknowledgment. J.E.K. acknowledges the National Research School Combination Catalysis for financial support.

Supporting Information Available: Static and dynamic light scattering data of **1**−**4** and **6**. Static and dynamic light scattering data of **2** as a function of time. Cryo-electron microscopy pictures of **1**, **2**, and **5**. This material is available free of charge via the Internet at http://pubs.acs.org.

References and Notes

(1) Zana, R. *Adv. Colloid Interface Sci.* **2002**, *97*, 205−253.
(2) Kirby, A. J.; Camilleri, P.; Engberts, J. B. F. N.; Feiters, M. C.; Nolte, R. J. M.; Söderman, O.; Bergsma, M.; Bell, P. C.; Fielden, M. L.; Rodriguez, C. L. G.; Guedat, P.; Kremer, A.; McGregor, C.; Perrin, C.; Ronsin, G.; van Eijk, M. C. P. *Angew. Chem., Int. Ed.* **2003**, *42*, 1448−1457.
(3) Bell, P. C.; Bergsma, M.; Dolbnya, I. P.; Bras, W.; Stuart, M. C. A.; Rowan, A. E.; Feiters, M. C.; Engberts, J. B. F. N. *J. Am. Chem. Soc.* **2003**, *125*, 1551−1558.
(4) Johnsson, M.; Engberts, J. B. F. N. *J. Phys. Org. Chem.* **2004**, *17*, 934−944.
(5) Klijn, J. E.; Scarzello, M.; Stuart, M. C. A.; Wagenaar, A.; Engberts, J. B. F. N. *Org. Biomol. Chem.* **2006**, *4*, 3569−3570.
(6) Scarzello, M.; Klijn, J. E.; Wagenaar, A.; Stuart, M. C. A.; Hulst, R.; Engberts, J. B. F. N. *Langmuir* **2006**, *22*, 2558−2568.
(7) Johnsson, M.; Wagenaar, A.; Stuart, M. C. A.; Engberts, J. B. F. N. *Langmuir* **2003**, *19*, 4609−4618.
(8) Alami, E.; Beinert, G.; Marie, P.; Zana, R. *Langmuir* **1993**, *9*, 1465−1467.
(9) Wettig, S. D.; Verrall, R. E. *J. Colloid Interface Sci.* **2001**, *235*, 310−316.
(10) Israelachvili, J. N.; Mitchell, D. J.; Ninham, B. W. *J. Chem. Soc., Faraday Trans. 2* **1976**, *72*, 1525−1568.
(11) Wagenaar, A.; Engberts, J. B. F. N., manuscript in preparation.
(12) Edwards, K.; Almgren, M.; Bellare, J.; Brown, W. *Langmuir* **1989**, *5*, 473−478.
(13) Almgren, M.; Edwards, K.; Karlsson, G. *Colloids Surf., A* **2000**, *174*, 3−21.
(14) Edwards, K.; Gustafsson, J.; Almgren, M.; Karlsson, G. *J. Colloid Interface Sci.* **1993**, *161*, 299−309.
(15) Silvander, M.; Karlsson, G.; Edwards, K. *J. Colloid Interface Sci.* **1996**, *179*, 104−113.
(16) Gustafsson, J.; Orädd, G.; Lindblom, G.; Olsson, U.; Almgren, M. *Langmuir* **1997**, *13*, 852−860.
(17) Gustafsson, J.; Orädd, G.; Almgren, M. *Langmuir* **1997**, *13*, 6956−6963.
(18) Size distributions were obtained by fitting a Gaussian function to intensity as a function of the logarithm of the particle diameter. The width of the size distribution is then the width at half-height.
(19) Siegel, D. P.; Green, W. J.; Talmon, Y. *Biophys. J.* **1994**, *66*, 402−414.
(20) Gustafsson, J.; Nylander, T.; Almgren, M.; Ljusberg-Wahren, H. *J. Colloid Interface Sci.* **1999**, *211*, 326−335.
(21) At high protonation states, mainly structures with high curvatures (low packing parameters) are formed. Hence, the *y*-axis ranges typically from 0 to about 0.5. At low protonation states, the structures with low curvatures (high packing parameters) are formed. Hence, the *y*-axis ranges typically from 0 to about 1.3.
(22) Close to the pH of the transition to worm-like micelles.
(23) Johnsson, M.; Wagenaar, A.; Engberts, J. B. F. N. *J. Am. Chem. Soc.* **2003**, *125*, 757−760.